Using Narrow and Wide Field of View Instruments to Evaluate Longwave Parameterizations for Fair Weather Cumulus Cloud Fields

E. E. Takara and R. G. Ellingson
Department of Meteorology
Florida State University
Tallahassee, Florida

Introduction

Full blown three-dimensional (3D) radiation calculations for broken cloud fields consume too much time and computing resources to be included in climate models. The 3D effects can be approximated by effective cloud fractions which reduce the three-dimensional calculation to an average of plane parallel solutions – a much easier problem.

For broken cloud conditions, the longwave flux (F) can be written as the weighted average of clear and overcast fluxes:

$$F = (1 - N_e)F_{clear} + N_e F_{overcast} \quad (1)$$

F_{clear} is the clear-sky flux; the flux that would occur if the broken cloud field was removed. $F_{overcast}$ is the flux that would occur if the broken cloud field became completely overcast. N_e is the fractional sky coverage of flat black plates.

Previous works (Ellingson, 1982; Killen and Ellingson 1994; Ellingson and Han 1999) gave N_e as a function of absolute cloud amount (N) and cloud aspect ratio (β):

$$N_e = N_e(N, \beta) \quad (2)$$

In this work, N_e derived from measurement is compared to sky cover measurements and N_e from parameterizations.

Instruments and Measurements

This work is based on measurements made at the Atmospheric Radiation Measurement (ARM) Southern Great Plains (SGP) Central Facility (CF) from April through June 1999. Six data streams from the ARM SGP central facility are used in this study. The active remote sensing clouds layer (ARSCL) boundary data is used in combination with wind profiler velocity data to derive N and β. The microwave radiometer (MWR) is used to indicate the presence of optically thick water clouds, acting as

a screen for the ARSCL data. The total sky imager (TSI) is used in an alternative derivation of N and also the hemispherical cloud cover. The atmospheric emitted radiance interferometer (AERI) measures the downwelling radiance at the surface from 520-1250cm^{-1} with high resolution. Pyrgeometers measure the longwave (0-3000cm^{-1}) downward flux at the surface. The millimeter wave cloud radar (MMCR), MWR, and AERI look directly upward with a small field of view; the pyrgeometers have a full hemispheric view.

Re-arranging (1) to solve for N_e yields:

$$N_e = \frac{F - F_{clear}}{F_{overcast} - F_{clear}} \tag{3}$$

F can be measured directly by the pyrgeometers. F_{clear} and $F_{overcast}$ are computed using the AERI spectral data and cloud base data from the Belfort baser ceilometer (BLC) or MMCR. In this way, N_e can be derived from measurements.

Computing F_{clear} and $F_{overcast}$

In order to compute F_{clear} and $F_{overcast}$ during a particular 24-hour period, occurrences of clear or overcast skies must be identified. The AERI is used for this purpose. The AERI radiance standard deviation in the 985-990cm^{-1} interval is a good indicator for clear or overcast skies; low standard deviations indicate either clear or overcast skies. High standard deviations indicate broken cloud fields. Overcast skies have high radiances and low standard deviations; clear skies have low radiances and low standard deviations. The clear and overcast AERI radiances are used to compute limiting values of clear and overcast radiance throughout the day. Computing the limiting values requires information on the changing conditions at both the surface and atmosphere. The AERI can provide this information because of its high spectral resolution.

Once clear and overcast measured radiances are identified, the clear and overcast radiances throughout the rest of the day can be estimated through an iteration process.

$$I_{AERI}^{overcast}(\text{estimated}) = \int_{833\text{cm}^{-1}}^{1250\text{cm}^{-1}} I(\nu, \text{observed overcast})d\nu + B_{opaque}(T_{surf}) \tag{4a}$$

$$I_{AERI}^{clear}(\text{estimated}) = \int_{833\text{cm}^{-1}}^{1250\text{cm}^{-1}} I(\nu, \text{observed clear})d\nu + B_{opaque}(T_{surf}) \tag{4b}$$

$$B_{opaque} = \int_{520\text{cm}^{-1}}^{833\text{cm}^{-1}} B(T_{surf}, \nu)d\nu + \int_{1250\text{cm}^{-1}}^{3000\text{cm}^{-1}} B(T_{surf}, \nu)d\nu \tag{4c}$$

The resulting envelopes of measured and estimated AERI radiances are used to compute the "AERI flux:"

$$F_{uncorrected} = LI_{AERI} + \pi \int_{0cm^{-1}}^{520cm^{-1}} B(T_{surf}, \nu)d\nu + \delta F_{offset} \quad (5)$$

For clear skies L = 3.45; for cloudy skies L ranges linearly from π at the surface to 3.25 at 6km. δF_{offset} is a correction factor to correct for AERI-pyrgeometer biases. δF_{offset} is found by averaging the difference between $F_{uncorrected}$ and the pyrgeometer flux for known clear and overcast.

Determining N, β, and Cloud Amount

β and one estimate of N were found using ARSCL and wind velocity data as described in Han and Ellingson (1999). Briefly, the ratio of the time a cloud was detected to the total measurement time is related to N. Assuming the clouds are advecting over the instruments at the wind velocity, the cloud diameter can be found. Combined with the ARSCL cloud thickness, the aspect ratio β is found. The MWR was used to screen out the atmospheric plankton and anomalous thin water clouds composed of large droplets.

The TSI cloud mask translating the original TSI image into a simple integer array with values indicating whether the matching pixel in the image is clear, cloudy, clear, unknown, or blocked.

Since mostly cloud bottoms are detected within small zenith angles, the number of cloudy pixels divided by the number of cloudy plus clear pixels of the cloud mask within a radius corresponding to the small zenith angle can be used to approximate N. In this study, a radius corresponding to 20 degrees was used:

$$N = \left. \frac{\#\,\text{cloudy pixels}}{\#\,\text{clear pixels} + \#\,\text{cloudy pixels}} \right|_{R \Rightarrow 20^{\circ}} \quad (6)$$

This is an alternative to the N derived from the fraction of time where clouds are detected discussed above.

A hemispherical cloud fraction (HCF) can defined the number of cloudy pixels divided by the number of clear plus cloudy pixels for the entire cloud mask:

$$HCF = \left. \frac{\#\,\text{cloudy pixels}}{\#\,\text{clear pixels} + \#\,\text{cloudy pixels}} \right|_{total} \quad (7)$$

Comparing N_e

Figures 1 shows N_e curves of the randomly overlapping cylinder parameterization in Ellingson 1982 and the data points corresponding to the ARSCL and MWR N and AERI retrieved N_e pairs in blue and the TSI derived N and AERI retrieved N_e pairs in red for July 22, 2000. The solid black curve is the randomly overlapping parameterization for the median cloud aspect ratio for the time interval considered on July 22, the dashed lines are for the highest and lowest cloud aspect ratios for that day. These are the upper and lower limits for the parameterization.

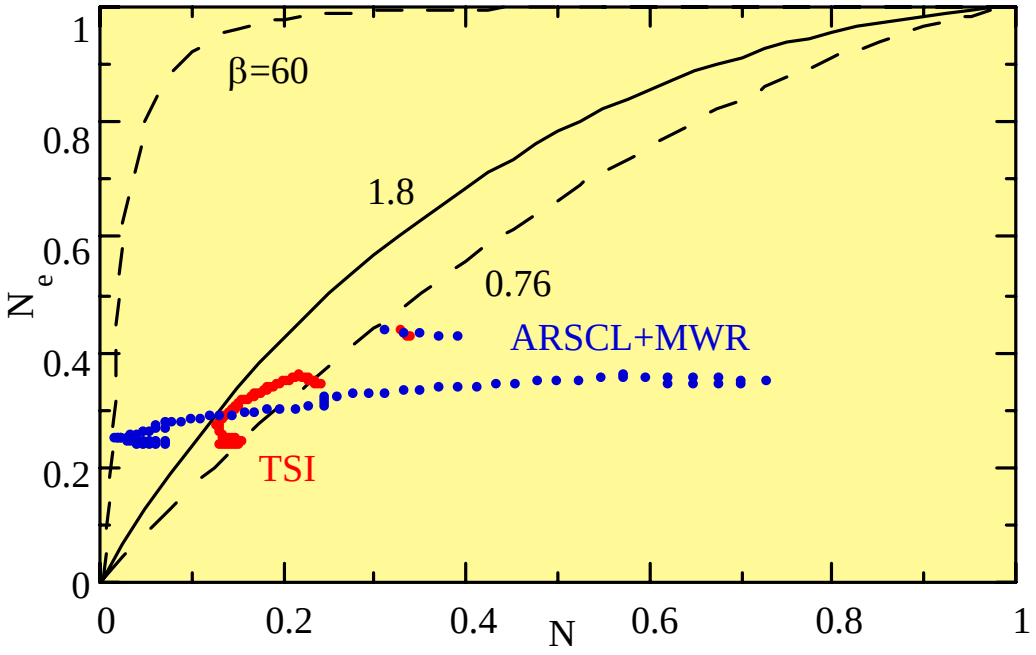

Figure 1. TSI N, AERI Ne, and ARSCL+MWR, AERI Ne pairs on July 22, 2000.

Since the y-coordinate (AERI N_e) is the same for both the blue and red points, the difference in the location on the graph is due entirely to the x-coordinate, the N derived from ARSCL and MWR and the TSI respectively. Note that the N derived from the TSI are grouped more closely together and demonstrated a higher degree of correlation with the AERI N_e. The ARSCL MWR derived N are quite scattered in comparison. This is due to the wider field of view (20º) for the TSI derived N; the ARSCL field of view is quite narrow in comparison. Since the TSI N sees more of the sky, it partially avoids the "pinhole" problem of whether the small fraction of the sky sampled by the narrow field of view instruments is representative for a given time interval.

Figure 2 shows the time series of the AERI N_e and the TSI HCF in Universal Time Coordinates (UTC). Considering the TSI is a daylight/shortwave instrument and the AERI N_e is derived from a set of longwave measurements the agreement is encouraging.

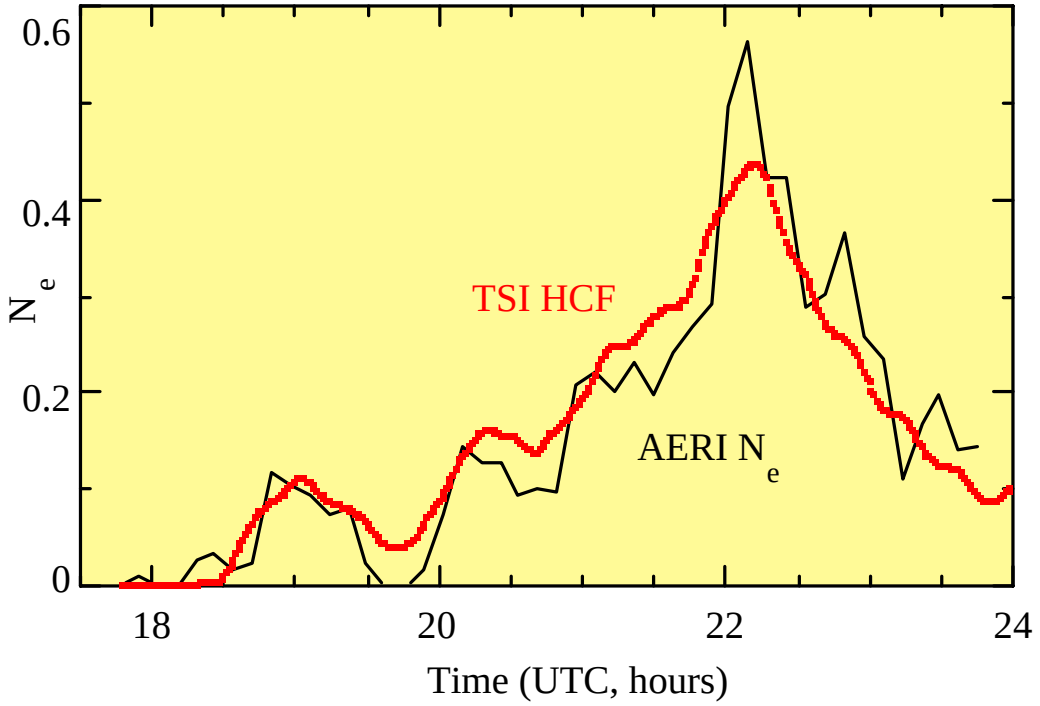

Figure 2. Time series for the TSI HCF (red) and the AERI Ne (black) on July 22, 2000.

Summary and Conclusions

A method for deriving the effective cloud fraction, N_e, from ARM measurements was presented. The derived N_e were combined with absolute cloud fractions, N, derived from two different sources: the MWR screened ARSCL and the TSI. The resulting comparison with the randomly overlapping cylinder parameterization showed that the N measured by the TSI is a significant improvement over the N from the MWR screened ARSCL. The N from the TSI showed a much higher correlation with the AERI N_e. Since it is a directly measured quantity, the TSI N can be considered more accurate. To improve the AERI derived Ne, the clear and overcast flux envelopes must be more accurate. The agreement between the AERI N_e and the TSI HCF is somewhat surprising and suggests that the AERI N_e can be used to provide a continuous day and night measurement of cloud cover by water clouds.

Acknowledgment

This paper was sponsored in part by the U.S. Department of Energy's Atmospheric Radiation Measurements Program under Grant DEFG0202ER63338.

Corresponding Author

Ezra Takara, etakara@met.fsu.edu, 850-644-3340

References

Ellingson, R. G., 1982: On the effects of cumulus dimensions on longwave irradiance and heating rates. *J. Atmos Sci*., **35**, 886-896.

Killen, R., and R. G. Ellingson, 1994: The effect of shape and spatial distribution of cumulus clouds on longwave irradiance. *J. Atmos. Sci*., **51**, 2123-2136.

Han, D. and R. G., 1999: Cumulus cloud parameterizations for longwave radiation calculations. *J. Atmos. Sci*., **56**, 837-851.